Dynamical Jahn-Teller Effects for a V^{3+} Ion in a MgO Crystal

T. Ray
Laboratoire de Spectrométrie Physique, Faculté des Sciences, 38, Grenoble, France
and Laboratoire de Physique des Solides, Faculté des Sciences, 91, Orsay, France
(Received 19 July 1971)

A theory of the acoustic paramagnetic resonance APR for V^{3+} ions in MgO is developed to explain the results of Brabin-Smith and Rampton which shows the importance of the second-order spin-orbit interaction resulting from Jahn-Teller interactions, i.e., from the excited vibronic levels. Essentially, it is this interaction which is responsible for lifting the degeneracy of the spin-orbit ground states $E_g + T_{2g}$ of the V^{3+} ions in the cubic state. Straightforward APR experiments give the g value within the excited triplet T_{2g} and the magnitude of the zero-field separation (D) between the T_{2g} and E_g levels is deduced from the study of the dependence of the APR spectra on temperature. The magnitudes of the Jahn-Teller energy E_{JT} and the frequency ω_E of the E_g mode of vibration of the molecular cluster formed around a V^{3+} ion, which give the best fit with the experimentally observed parameters g and D, are in good agreement with the estimate of E_{JT} in an effective point-charge model and with the results on phonon sidebands in MgO crystals doped with different paramagnetic impurities, respectively. The strongly asymmetric nature of the line shape is explained by taking into account the presence of small random strain fields of tetragonal and orthorhombic nature about the cubic site. The experimentally determined hyperfine parameter A is fitted in this theory, assuming the magnitude of the contact term k to be 0.2.

I. INTRODUCTION

The V^{3+} ion in a MgO crystal is an interesting system to study because it is a non-Kramers ion having a triply degenerate (T_{1g}) orbital ground level and consequently, the Jahn-Teller interaction is expected to have pronounced effects on the magnetic and other related properties. Brabin-Smith and Rampton[1] have studied the acoustic paramagnetic resonance (APR) in this system and in the present paper, a theory is given to explain their observations. With the Zeeman field along [100] and the ultrasonic waves propagating along [100], a broad asymmetric resonance line was observed which showed hyperfine structure on its high-field side due to the nuclear spin $I = \frac{7}{2}$. From an examination of the temperature dependence of the spectra between 14 and 20 °K, it was inferred that the resonance line was due to the transitions induced within excited spin-orbit states which lie (10.2 ± 1.0) cm^{-1} above the ground level. The transition corresponded to the selection rule $\Delta m_s = \pm 2$. The g value and the hyperfine-interaction parameter A were found to be 0.69 ± 0.01 and 0.0042 cm^{-1}, respectively. The resonance spectrum was assumed to be due to an excited spin-orbit doublet of the V^{3+} ions at the tetragonal sites in MgO. With the Zeeman field still along [100] but the acoustic waves propagating along [110] the same resonance line was observed.

A theory was proposed by Bates, Goodfellow, and Stevens[2] to explain these experimental observations for V^{3+} ions in the MgO lattice. Essentially they proposed that the spectra are due to the V^{3+} ions at the tetragonal sites in the MgO crystal and they obtained a numerical fit of the experimental results by taking into account the Jahn-Teller reduction of the spin-orbit coupling parameter λ within the ground T_{1g} levels. According to their theory, the resonance is caused within an excited spin-orbit doublet, which is separated from the nonmagnetic ground levels by the action of the tetragonal field, i.e., the zero-field separation D is entirely due to the tetragonal field. Starting with a spin-orbit coupling parameter $\lambda = 85$ cm^{-1} (the free-ion value of which is 104 cm^{-1}) and taking the g value to be $0.69 + 0.035$ (where the positive contribution was added to correct the experimental result for the effects of rhombic strains), they predicted the tetragonal field Δ to be of the order of 8.7 cm^{-1} and a Jahn-Teller reduction factor[3] $k(T_1) = 0.15$, in order to obtain a plausible energy-level diagram which would explain the observations. These values give an excited doublet at 3.8 cm^{-1} above the nonmagnetic ground levels at zero field, which is significantly different from the experimental value. Besides some obscure points in the details of this analysis, the model itself is quite inadequate from physical reasonings. First, the existence of a definite tetragonal field of such a small magnitude as they obtain, raises questions about its physical origin. Second, nothing in the theory tells us what happens to the V^{3+} ions in the cubic sites—what role do they play in the resonance spectra? Third, in view of the strong reduction in the spin-orbit coupling parameter, as they predict, which envisages a strong Jahn-Teller interaction, one would expect the second-order spin-orbit inter-

action due to the excited vibronic levels to be important[3] and no conclusion could be made on the basis of the first-order spin-orbit Hamiltonian as used by Bates *et al.*[2] Actually, it can be shown that the solution of this Hamiltonian does not give an unique set of values for λ and $k(T_1)$ and one could explain quantitatively the observed values of g and D even with an unquenched spin-orbit parameter λ and a different value of the tetragonal field Δ. Also, the model of Bates *et al.* does not explain the unusually asymmetric line shape of the observed APR spectra.

In the present paper, a theory of the APR of V^{3+} ions in a MgO crystal is developed which brings into evidence the important role played by the excited vibronic levels in splitting the vibronic spin-orbit ground states of V^{3+} ions at the cubic sites. The spin-orbit interaction within the vibronic triplet ground state (T_{1g}) causes only a reduction $k(T_1)$ in the spin-orbit interaction parameter λ and gives rise to a fivefold degenerate lowest level ($T_{2g}+E_g$). It is shown here that further splitting of this fivefold level into a nonmagnetic doublet state E_g and an excited triplet state T_{2g} is caused by the effect of the excited vibronic levels on the vibronic triplet ground state T_{1g}, i.e., through the second-order spin-orbit interactions. Thus V^{3+} ions in MgO seem to be an unique example where the importance of the vibronically induced spin-orbit interaction is manifest in lifting the degeneracy of the spin-orbit ground states which were otherwise accidentally degenerate. This is in contrast to other cases of ions like Co^{2+} [4] and Fe^{2+} [5] in MgO with an orbital triplet lowest level in which the Jahn-Teller effects have been studied so far. It is the excited triplet T_{2g} within which the acoustic resonance is observed and by studying the intensity of the resonance absorption as a function of temperature one would obtain the separation between this triplet from the doublet ground state E_g. The assumption of Brabin-Smith and Rampton that the orbital triplet state T_{1g} is relatively weakly coupled to the T_{2g} modes of vibration of the molecular cluster formed by the six O^{2-} ions surrounding the V^{3+} impurity ion, is substantiated by our calculations based on an effective point-charge model. So in our present calculations the coupling of the T_{1g} level with only the E_g modes of vibration has been considered. The zero-field separation between the T_{2g} and E_g levels and the g value within the T_{2g} triplet state are expressed in terms of E_{JT}, the Jahn-Teller energy due to the coupling with the E_g modes of vibration and ω_E, the frequency of these modes of vibration. The values of E_{JT} and $\hbar\omega_E$ thus determined by comparing with the experimental values of g and D are in reasonably good agreement with the value of E_{JT} calculated on an effective point-charge model and that of $\hbar\omega_E$ obtained from experimental results on phonon sidebands for different paramagnetic ions in MgO.[6]

The APR spectra of the V^{3+} ions in MgO are thus shown to be due to the V^{3+} ions at cubic sites and the experimental g value and the zero-field separation D are well explained on the basis of this model. But to explain the very broad and unusually asymmetric line shape, one has to take into account the effects of the random strain fields of tetragonal and orthorhombic types about the cubic sites. The presence of the distortion divides the total number of impurity ions into three groups, depending on whether the tetragonal axis is parallel or orthogonal to the Zeeman field. It will be seen that for all three groups of ions, only one resonance absorption can be detected easily whose peak is at $g=g_{\text{cubic}}$. This resonance corresponds to $\Delta m_s=\pm 2$ transitions for the ions with the tetragonal axis parallel to the magnetic field. The magnitude of the hyperfine interaction is also well explained in this theory assuming a fairly reasonable value of the contact interaction term.

We now present the details of this work starting with an account of the theory based on the assumption that the APR spectra in $MgO:V^{3+}$ are due to a definite static tetragonal distortion. In Sec. II, we discuss the consequences of this assumption taking the spin-orbit interaction in its first order only, i.e., within the triplet ground state T_{1g}. We discuss the theory of the Jahn-Teller interaction for V^{3+} ions at the cubic sites in Sec. III, and in Sec. IV this theory is extended to include the effects due to the presence of a small random strain field of tetragonal nature about the cubic sites. The relative strengths of the coupling of the orbital level T_{1g} with the E_g and the T_{2g} modes of vibration of the molecular cluster and also the Jahn-Teller energy E_{JT} are calculated with an effective point-charge model in the Appendix. The conclusions are summarized and general discussions are included in Sec. V.

II. THEORY OF APR OF V^{3+} IN MgO ON ASSUMPTION OF STATIC TETRAGONAL DISTORTION AND TAKING SPIN-ORBIT INTERACTION WITHIN GROUND-STATE TRIPLET ONLY

The V^{3+} ion is of $3d^2$ configuration and has a ^3F lowest term. The ionic levels are shown in Fig. 1. The optical absorption spectra given by Sturge[7] indicate that the vanadium ion in the triply ionized state enters substitutionally in a MgO crystal and the ^3F term splits up into two triplets $^3T_{1g}$ and $^3T_{2g}$ and a singlet $^3A_{2g}$, the triplet $^3T_{1g}$ being the lowest. Any transitions within the ^3F and the ^1D terms are spin forbidden but there is admixing of the $^3T_{1g}$ level due to the ^3P term and the ground $^3T_{1g}$ level by the cubic crystal field. Denoting the separation between the ^3F and the ^3P terms by $15B$, where B is the appropriate Racah integral,[8]

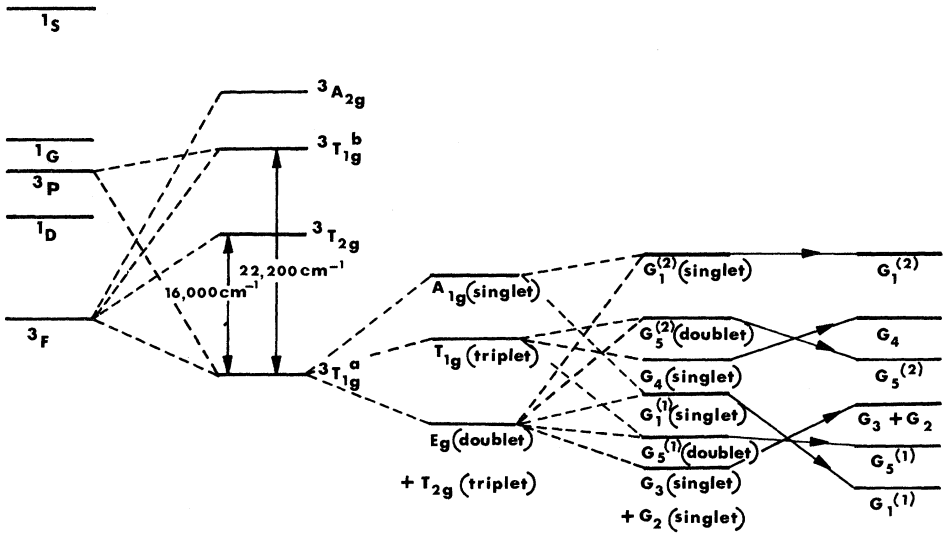

FIG. 1. The low-lying electronic energy levels of the V^{3+} ion in MgO with spin-orbit interaction and static tetragonal field. The cubic representations follow Mulliken's notation and for the tetragonal representations we have used G_i's.

we get the following expressions for the energies of the different levels in the cubic crystal field:

$$E(^3T_{1g}^a) = 0.5\{(15B - 6Dq) - [(15B + 6Dq)^2 + 64D^2q^2]^{1/2}\},$$

$$E(^3T_{2g}) = 2Dq\ , \quad E(^3A_{2g}) = 12Dq\ , \tag{1}$$

$$E(^3T_{1g}^b) = 0.5\{(15B - 6Dq) + [(15B - 6Dq)^2 + 64D^2q^2]^{1/2}\},$$

where Dq is the usual cubic field parameter. Associating the observed optical spectra of the transitions $^3T_{1g}^a \rightarrow {}^3T_{2g}$ and $^3T_{1g}^a \rightarrow {}^3T_{1g}^b$, we get $Dq = 1707$ cm^{-1} and $B = 484.66$ cm^{-1}. It is to be noted that this value of Dq is of the same order as that obtained by Pryce and Runciman[9] for the case of V^{3+} in Al_2O_3, whereas the parameter B is much reduced. The net effect of the mixing of F and P terms in the lowest T_{1g} level is to change the value of the effective angular momentum within this triplet. The orbital ground state $^3T_{1g}^a$ is given by

$$T_{1g}^a = T_{1g}(F)\cos\theta + T_{1g}(P)\sin\theta\ , \tag{2}$$

where

$$\tan\theta = -[(6Dq + 15B) + (225B^2 + 180BDq + 100D^2q^2)^{1/2}]\ .$$

The angular-momentum operator $\vec{l}$ within the orbital triplet is given by $\vec{L} = \alpha\vec{l}$, where $\alpha = -1.5 \times (\cos^2\theta + \frac{2}{3}\sin^2\theta)$ and L is the orbital angular momentum of the F term and has the value 3. With the values of B and Dq obtained from the optical data, α comes out to be -1.2. When the mixing between F and P terms is neglected α is -1.5. A reduction factor K due to the covalency effects should also be taken into account so that $\vec{L} = \alpha K\vec{l}$. When vibronic interactions are considered so that the triplet ground state is vibronic rather than electronic, there will be an additional Ham reduction factor.

We shall now examine the consequences of the hypothesis that the APR spectra of $MgO:V^{3+}$ are due to the combined effects of a tetragonal field and the spin-orbit interaction, effective only within the triplet ground state. On this supposition the perturbing Hamiltonian of the system is

$$\mathcal{H} = \mathcal{H}_{so}^{(1)} + \mathcal{H}_T\ , \tag{3}$$

where

$$\mathcal{H}_{so}^{(1)} = \lambda_{eff}\vec{l}\cdot\vec{s}$$

and

$$\mathcal{H}_T = -\Delta[l_z^2 - \tfrac{1}{3}l(l+1)]\ . \tag{4}$$

By $\mathcal{H}_{so}^{(1)}$ we denote the spin-orbit interaction in its

first order where all the excited levels are excluded from consideration. The tetragonal field splits up the orbital triplet ground state into a doublet and a singlet, the singlet lying Δ cm^{-1} above or below the doublet depending on whether Δ is positive or negative.

The energy-level diagram under the action of these perturbing interactions [Eq. (3)] is drawn schematically in Fig. 1 for both positive and negative values of Δ. For positive Δ, the lowest level is a nonmagnetic doublet (the degeneracy is accidental) with another doublet as the first-excited level, as has been found by Bates *et al.* For negative Δ, the doublet is still the first-excited level but the lowest level is a singlet. The separation of the first-excited doublet from the ground-state level is given by

$$D = -\tfrac{1}{3}\lambda_{\text{eff}}[3+y-(9+y^2)^{1/2}] \quad \text{for positive } \Delta$$

and (5)

$$D = -\tfrac{1}{3}\lambda_{\text{eff}}[-\tfrac{3}{2}-(9+y^2)^{1/2}+(729+36y^2-108y)^{1/2}]$$

for negative Δ,

where

$$y = -3\Delta/2\lambda_{\text{eff}} .$$

Taking this doublet to be the $|\pm 1\rangle$ states of an effective spin $S=1$, we get the following expression for $g_{\parallel}$:

$$g_{\parallel} = \tfrac{1}{4}\cos^2\beta[-2\alpha K(1+\tan\beta)^2 - 4(1-\tan\beta)^2] , \quad (6)$$

where

$$\tan\beta = 3/y + (9/y^2+1)^{1/2} .$$

It should be noted that $\lambda_{\text{eff}} = \alpha K \lambda_{\text{free ion}}$, where K takes into account any reduction in λ from the free-ion value due to covalency effects. The multiplying factor α has been defined above. Taking the free-ion value to be 104 cm^{-1},[10] one obtains $\lambda_{\text{eff}} = -125$ cm^{-1} if no reduction is considered. At one end of the scale, when K is taken to be nearly unity one gets $D = 6.63$ cm^{-1} and $g = 0.69$ for $\lambda_{\text{eff}} = -120$ cm^{-1} and $\Delta = -45$ cm^{-1}. At the other end of the scale one gets $D = 3.7$ cm^{-1} and $g = 0.70$ for $\lambda_{\text{eff}} = -24$ cm^{-1} and $\Delta = 8.0$ cm^{-1}. And in between there are a number of different sets of values of λ_{eff} and Δ, with which similar quantitative agreement with the experimental values of g and D is obtained. Remembering that our definition of λ_{eff} includes the factor $-\frac{3}{2}$, it can be seen that the latter set of quoted values is nearly the same as that given by Bates *et al.* With the Hamiltonian in Eq. (3) one never really attains a simultaneous good fit with the experimental values of D and g as given by Brabin-Smith and Rampton. Even if one overlooks this quantitative disagreement, one cannot be satisfied with the assumption that the spectra are due to V^{3+} ions in tetragonal sites because of the following difficulties:

(i) If one assumes no reduction or a very small reduction in the value of λ then to get a close fit of the experimental results one finds that the magnitude of the tetragonal field is somewhat large but not so large as to be explained by charge-compensation processes,[11] although the sign seems to be correct. However, it is highly improbable that λ will remain unquenched in $MgO:V^{3+}$, in view of the fact that the vibronic interactions should be important in this system.

(ii) On the other hand, if a sufficient reduction in λ is taken into account then the magnitude of the tetragonal field comes out to be very small. It is not clear what mechanism can give rise to such small but definite value of Δ. Also, a large reduction in the spin-orbit parameter can only be explained in terms of a fairly strong Jahn-Teller coupling, in which case, no conclusion can be arrived at before one investigates the second-order effect of the vibronically induced spin-orbit interaction.

(iii) Whatever may be the origin of the tetragonal field, there should be a large number of V^{3+} ions in the cubic sites and no theory is complete unless one knows what is the nature of the spectra from these sites. Also, the very asymmetric line shape of the observed spectra has to be correctly explained.

III. THEORY OF THE DYNAMIC JAHN-TELLER EFFECTS IN V^{3+} IONS AT CUBIC SITES

The V^{3+} ion in the MgO lattice has an extra positive charge compared to that of the host ion Mg^{2+} and as a result, the extra charge would be compensated by the creation of a positive ion vacancy near the V^{3+} ion as in the case of Cr^{3+} in MgO.[12] But one positive ion vacancy at the Mg^{2+} site will compensate for the extra charges on two V^{3+} ions, one of which is local and the other nonlocal. For the local V^{3+} ion, the vacancy would produce a crystal field of symmetry lower than cubic whereas for the distant ion the symmetry would still be cubic. So one expects equal numbers of V^{3+} ions in cubic and noncubic sites. In this section we shall study the nature of the APR spectra of the V^{3+} ions at the cubic sites taking the Jahn-Teller interactions into consideration.

For the V^{3+} ions in the cubic site the total Hamiltonian is

$$\mathcal{H} = \mathcal{H}_{\text{ion}} + \mathcal{H}_{\text{cubic}} + \mathcal{H}_{\text{lattice}} + \mathcal{H}_{\text{vib}} + \mathcal{H}_{\text{so}} + \mathcal{H}_{g} + \mathcal{H}_{hf} . \quad (7)$$

The energy levels of the first two terms of the above Hamiltonian have already been described in Sec. II and are shown schematically in Fig. 1. As the first-excited orbital level $^3T_{2g}$ is 16 000 cm^{-1} above the ground $^3T_{1g}^a$ level[7] in this section we shall

confine ourselves exclusively to the ground-state triplet.

A. Orbit-Lattice Interaction

In problems of paramagnetic ions in crystals, the nearest-neighbor model has been shown[3,13] to be adequate for describing the orbit-lattice interactions and the only relevant modes of vibration of the molecular cluster formed by the six O^{2-} ions surrounding the impurity ion with which the orbital triplet ${}^3T_{1g}^a$ will interact are the E_g and T_{2g} modes. Thus, following the notations used by Ham,[3] we have

$$\mathcal{H}_{\text{lattice}} = [(1/2\mu)(P_\theta^2+P_\epsilon^2)+\tfrac{1}{2}\mu\omega_E^2(Q_\theta^2+Q_\epsilon^2)]\,\mathcal{I} + [(1/2\mu)(P_\xi^2+P_\eta^2+P_\zeta^2) + \tfrac{1}{2}\mu\omega_T^2(Q_\xi^2+Q_\eta^2+Q_\zeta^2)] \quad (8)$$

and

$$\mathcal{H}_{\text{vib}} = V_E(Q_\theta\,\mathcal{E}_\theta + Q_\epsilon\,\mathcal{E}_\epsilon) + V_T(Q_\xi\,\mathcal{T}_\xi + Q_\eta\,\mathcal{T}_\eta + Q_\zeta\,\mathcal{T}_\zeta)\,, \quad (9)$$

where P and Q denote the momentum and the symmetry adapted displacement coordinates. θ and ϵ are the two components of E_g modes of vibration, and ξ, η, and ζ are the three components of the T_{2g} modes of vibration, ω_E and ω_T denoting, respectively, their average frequency. μ is the effective mass of the modes which in the molecular cluster model is equivalent to the mass of the O^{2-} ion.[3] V_E and V_T are the coupling coefficients for the E_g and T_{2g} modes, respectively, with the T_{1g} orbital states. The three components of the electronic T_{1g} ground level are denoted by $|X\rangle$, $|Y\rangle$, and $|Z\rangle$ and the matrices $\mathcal{I}$, $\mathcal{E}$, and $\mathcal{T}$ defined with respect to these states are given by

$$\mathcal{I} = \begin{pmatrix} 1 & 0 & 0 \\ 0 & 1 & 0 \\ 0 & 0 & 1 \end{pmatrix}, \qquad \mathcal{E}_\theta = \begin{pmatrix} \frac{1}{2} & 0 & 0 \\ 0 & \frac{1}{2} & 0 \\ 0 & 0 & -1 \end{pmatrix},$$

$$\mathcal{E}_\epsilon = \begin{pmatrix} -\frac{1}{2}\sqrt{3} & 0 & 0 \\ 0 & \frac{1}{2}\sqrt{3} & 0 \\ 0 & 0 & 0 \end{pmatrix},$$

$$\mathcal{T}_\xi = \begin{pmatrix} 0 & 0 & 0 \\ 0 & 0 & -1 \\ 0 & -1 & 0 \end{pmatrix}, \quad \mathcal{T}_\eta = \begin{pmatrix} 0 & 0 & -1 \\ 0 & 0 & 0 \\ -1 & 0 & 0 \end{pmatrix}, \quad (10)$$

and

$$\mathcal{T}_\zeta = \begin{pmatrix} 0 & -1 & 0 \\ -1 & 0 & 0 \\ 0 & 0 & 0 \end{pmatrix}.$$

The expression for $\mathcal{H}_{\text{vib}}$ is simplified in the present case because V_T is much smaller than V_E as we shall see in the Appendix and consequently one can neglect the coupling with the T_{2g} modes. Considering $\mathcal{H}_{\text{lattice}}$ and $\mathcal{H}_{\text{vib}}$ for the E_g modes only we can construct the vibronic states which have the following eigenvalues and eigenfunctions:

$$E_{in_\theta n_\epsilon} = E_0 - E_{JT} + (n_\theta + n_\epsilon + 1)\,\hbar\omega_E$$

and (11)

$$|in_\theta n_\epsilon\rangle = |i\rangle\, F_{n_\theta}(Q_\theta + a_{i\theta})\, F_{n_\epsilon}(Q_\epsilon + a_{i\epsilon})\,,$$

where E_0 is the energy of the electronic triplet T_{1g}^a whose components $|i\rangle$ stand for $|X\rangle$, $|Y\rangle$, and $|Z\rangle$. The vibrational quantum numbers n_θ and n_ϵ can have values 0, 1, 2, 3, ... The Jahn-Teller energy E_{JT} is given by $V_E^2/2\mu\omega_E^2$. $F(Q)$ is the one-dimensional simple harmonic wave function. $a_{i\theta}$ and $a_{i\epsilon}$ are defined as

$$a_{i\theta} = V_E\, e_{i\theta}/\mu\omega_E^2\,, \quad a_{i\epsilon} = V_E\, e_{i\epsilon}/\mu\omega_E^2\,, \quad (12)$$

where $e_{i\theta}$ and $e_{i\epsilon}$ are the diagonal matrix elements of $\mathcal{E}_\theta$ and $\mathcal{E}_\epsilon$, respectively, given in Eqs. (10).

The vibronic ground levels which still form a triplet state are denoted by $|X00\rangle$, $|Y00\rangle$, and $|Z00\rangle$, and the vibronic excited levels $|in_\theta n_\epsilon\rangle$ are $(n_\theta+n_\epsilon)\,\hbar\omega_E$ cm^{-1} above the triplet. From the experiments on phonon sidebands in MgO crystals doped with different paramagnetic impurities one finds that $\hbar\omega_E$ is of the order of 400 cm^{-1},[6] and we have already seen that the maximum value of $|\lambda_{\text{eff}}|$ is 125 cm^{-1}. Hence we can take the spin-orbit interaction as a perturbation on the vibronic states. The perturbation procedure is further justified because $E_{JT} > |\lambda_{\text{eff}}|$, as will be shown later on.

B. Spin-Orbit Interaction

Within the vibronic ground triplet state, the $\mathcal{H}_{\text{so}}$ or more correctly $\mathcal{H}_{\text{so}}^{(1)}$ is given by

$$\mathcal{H}_{\text{so}}^{(1)} = \lambda_g\, \vec{l}_g \cdot \vec{s}\,, \quad (13)$$

where l_g is the orbital angular momentum within the vibronic triplet and is given by

$$\lambda_g = \lambda_{\text{eff}}\langle X00\,||\,(l)_1\,||\,Y00\rangle / \langle X00\,||\,(l_g)_1\,||\,Y00\rangle = \lambda_{\text{eff}}\exp(-\tfrac{3}{2}x),$$

where

$$x = E_{JT}/\hbar\omega_E\,. \quad (14)$$

Thus if we consider the vibronic ground triplet state only, then the degeneracies of the spin-orbit states will not change from that which we obtained earlier in the pure electronic case without taking account of the lattice vibrations. The eigenvalues and hence the energy separations of these states will change due to the new spin-orbit interaction parameter λ_g. The vibronic spin-orbit states and their spin-orbit energies are

$$
\begin{aligned}
E_g&: \left\{ \begin{array}{l} \frac{1}{\sqrt{6}}\,(2|Z00\rangle\,|s_z\rangle - |X00\rangle\,|s_x\rangle - |Y00\rangle\,|s_y\rangle) \\ \frac{1}{\sqrt{2}}\,(|X00\rangle\,|s_x\rangle - |Y00\rangle\,|s_y\rangle) \end{array} \right\} && \text{energy} \\
& && \lambda_g \\
T_{2g}&: \left\{ \begin{array}{l} \frac{1}{\sqrt{2}}\,(|Y00\rangle\,|s_z\rangle + |Z00\rangle\,|s_y\rangle) \\ \frac{1}{\sqrt{2}}\,(|X00\rangle\,|s_z\rangle + |Z00\rangle\,|s_x\rangle) \\ \frac{1}{\sqrt{2}}\,(|Y00\rangle\,|s_x\rangle + |X00\rangle\,|s_y\rangle) \end{array} \right\} && \lambda_g \\
T_{1g}&: \left\{ \begin{array}{l} \frac{1}{\sqrt{2}}\,(|Y00\rangle\,|s_z\rangle - |Z00\rangle\,|s_y\rangle) \\ \frac{1}{\sqrt{2}}\,(|Z00\rangle\,|s_x\rangle - |X00\rangle\,|s_z\rangle) \\ \frac{1}{\sqrt{2}}\,(|X00\rangle\,|s_y\rangle - |Y00\rangle\,|s_x\rangle) \end{array} \right\} && -\lambda_g \\
A_{1g}&: \frac{1}{\sqrt{3}}\,(|X00\rangle\,|s_x\rangle + |Y00\rangle\,|s_y\rangle + |Z00\rangle\,|s_z\rangle) && -2\lambda_g\ ,
\end{aligned}
\tag{15}
$$

where the spin states $|s_x\rangle$, $|s_y\rangle$, and $|s_z\rangle$ are given by

$$
\begin{aligned}
|s_x\rangle &= -\frac{1}{\sqrt{2}}\,(|1\rangle - |-1\rangle)\ , \\
|s_y\rangle &= \frac{i}{\sqrt{2}}\,(|1\rangle + |-1\rangle)\ , \\
|s_z\rangle &= |0\rangle\ ,
\end{aligned}
\tag{16}
$$

in terms of $|m_s\rangle$ states. Next, we consider the perturbing effects of the vibronic excited states $|Xn_\theta n_\epsilon\rangle$, $|Yn_\theta n_\epsilon\rangle$, and $|Zn_\theta n_\epsilon\rangle$ on the vibronic triplet ground state $|X00\rangle$, $|Y00\rangle$, and $|Z00\rangle$ through the spin-orbit coupling. The effective second-order spin-orbit Hamiltonian due to these vibronic excited levels is[3]

$$
\begin{aligned}
\mathcal{H}_{so}^{(2)} = &-\lambda_1(l_{gx}^2 s_x^2 + l_{gy}^2 s_y^2 + l_{gz}^2 s_z^2) - \lambda_2(l_{gx}l_{gy}s_x s_y \\
&+ l_{gy}l_{gx}s_y s_x + l_{gy}l_{gz}s_y s_z + l_{gz}l_{gy}s_z s_y \\
&+ l_{gz}l_{gx}s_z s_x + l_{gx}l_{gz}s_x s_z)\ ,
\end{aligned}
\tag{17}
$$

where

$$
\begin{aligned}
\lambda &= (\lambda_{\text{eff}}^2/\hbar\omega_E)\exp(-3x)\,G(3x) \\
\text{and} \\
\lambda_2 &= (\lambda_{\text{eff}}^2/\hbar\omega_E)\exp(-3x)\,G(3x/2)\ .
\end{aligned}
\tag{18}
$$

It can easily be shown that in the present case where the spin is unity, the form of the effective spin-orbit Hamiltonian remains the same as given in Eq. (17) if higher-order terms are considered. But it is sufficient if we consider the interaction up to the second order, because for higher-order terms the parameters λ_1 and λ_2 will be very small as both E_{JT} and $\hbar\omega_E$ are much larger than λ_{eff}. This effective Hamiltonian will lift the degeneracy between the E_g and T_{2g} levels and will cause shifts in the energies of the other levels. The modified spin-orbit energies are

$$
\begin{aligned}
E_g &: \lambda_g - 2\lambda_1 + \lambda_2\ , \\
T_{2g} &: \lambda_g - \lambda_1\ , \\
T_{1g} &: -\lambda_g - \lambda_1\ , \\
A_{1g} &: -2\lambda_g - 2\lambda_1 - 2\lambda_2\ .
\end{aligned}
\tag{19}
$$

Thus the separation of the excited triplet from the nonmagnetic ground doublet is $\lambda_1 - \lambda_2$. The vibronic spin-orbit energy levels are shown schematically in Fig. 2.

It should be mentioned here that the mixing of the vibronic excited levels through spin-orbit interaction will modify the T_{2g} spin-orbit states [Eq. (15)] to the following expressions:

$$
|T_{2g}^1\rangle = \frac{1}{\sqrt{2}}\,[\,|Y00\rangle\,|s_z\rangle + |Z00\rangle\,|s_y\rangle\,] + \frac{1}{\sqrt{2}}\sum_{n_\theta n_\epsilon}{}'\,[C_1(n_\theta n_\epsilon)|Zn_\theta n_\epsilon\rangle\,|s_y\rangle + C_2(n_\theta n_\epsilon)|Yn_\theta n_\epsilon\rangle\,|S_z\rangle\,]\ ,
$$

$$|T_{2g}^2\rangle = \frac{1}{\sqrt{2}}\left[|Z00\rangle|s_z\rangle + |X00\rangle|s_z\rangle\right] + \frac{1}{\sqrt{2}}\sum_{n_\theta n_\epsilon}{}' \left[C_3(n_\theta n_\epsilon)|Xn_\theta n_\epsilon\rangle|S_z\rangle + C_4(n_\theta n_\epsilon)|Zn_\theta n_\epsilon\rangle|S_x\rangle\right],$$

$$|T_{2g}^3\rangle = \frac{1}{\sqrt{2}}\left[|X00\rangle|S_y\rangle + |Y00\rangle|S_x\rangle\right] + \frac{1}{\sqrt{2}}\sum_{n_\theta n_\epsilon}{}' \left[C_5(n_\theta n_\epsilon)|Yn_\theta n_\epsilon\rangle|S_x\rangle + C_5(n_\theta n_\epsilon)|Xn_\theta n_\epsilon\rangle|S_y\rangle\right], \quad (20)$$

where

$$C_1 = -\frac{\lambda_{\text{eff}}}{\hbar\omega_E}\frac{A_+(\theta)B_-(\epsilon)}{n_\theta + n_\epsilon}\exp(-\tfrac{3}{2}x),$$

$$C_2 = -\frac{\lambda_{\text{eff}}}{\hbar\omega_E}\frac{A_-(\theta)B_-(\epsilon)}{n_\theta + n_\epsilon}\exp(-\tfrac{3}{2}x),$$

$$C_3 = -\frac{\lambda_{\text{eff}}}{\hbar\omega_E}\frac{A_-(\theta)B_+(\epsilon)}{n_\theta + n_\epsilon}\exp(-\tfrac{3}{2}x), \quad (21)$$

$$C_4 = -\frac{\lambda_{\text{eff}}}{\hbar\omega_E}\frac{A_+(\theta)B_-(\epsilon)}{n_\theta + n_\epsilon}\exp(-\tfrac{3}{2}x),$$

$$C_5 = -\frac{\lambda_{\text{eff}}}{\hbar\omega_E}\frac{1}{n_\epsilon}\left(\frac{1}{n_\epsilon!}\right)^{1/2}\left(-\sqrt{\tfrac{3}{2}}\frac{V_E\rho}{\mu\omega^2}\right)^{n_\epsilon}\exp(-\tfrac{3}{2}x),$$

$$C_6 = \frac{\lambda_{\text{eff}}}{\hbar\omega_E}\frac{1}{n_\epsilon}\left(\frac{1}{n_\epsilon!}\right)^{1/2}\left(\sqrt{\tfrac{3}{2}}\frac{V_E\rho}{\mu\omega^2}\right)^{n_\epsilon}\exp(-\tfrac{3}{2}x),$$

and

$$A_\pm(\theta) = (n_\theta!)^{-1/2}\left(\pm\frac{3}{2\sqrt{2}}\frac{V\rho}{\mu\omega^2}\right)^{n_\theta},$$

$$B_\pm(\epsilon) = (n_\epsilon!)^{-1/2}\left(\pm\frac{3}{2\sqrt{2}}\frac{V\rho}{\mu\omega^2}\right)^{n_\epsilon},$$

$$\rho = (\mu\omega/\hbar)^{1/2}.$$

The summation $\sum'_{n_\theta n_\epsilon}$ indicates that n_θ and n_ϵ cannot be simultaneously zero.

C. Zeeman Interaction

We now consider the effect of the Zeeman field on the vibronic spin-orbit states. In analogy with the spin-orbit interaction we can write down the effective Zeeman interaction for the vibronic triplet ground state as

$$\mathcal{H}_z = \mathcal{H}_z^{(1)} + \mathcal{H}_z^{(2)}, \quad (22)$$

where $\mathcal{H}_z^{(1)}$ stands for the Zeeman interactions on the vibronic triplet ground state neglecting the vibronic excited states and $\mathcal{H}_z^{(2)}$ is the additional second-order term which takes into account the mixing of these excited levels with the triplet ground state through spin-orbit interaction. These are given by

$$\mathcal{H}_z^{(1)} = \beta\vec{H}\cdot(\gamma\vec{l}_g + 2\vec{s}),$$

where

$$\gamma = \alpha K\exp(-3x/2) \quad (23)$$

and

$$\mathcal{H}_z^{(2)} = g_1\beta(l_{gx}^2 s_x H_x + l_{gy}^2 s_y H_y + l_{gz}^2 s_z H_z)$$

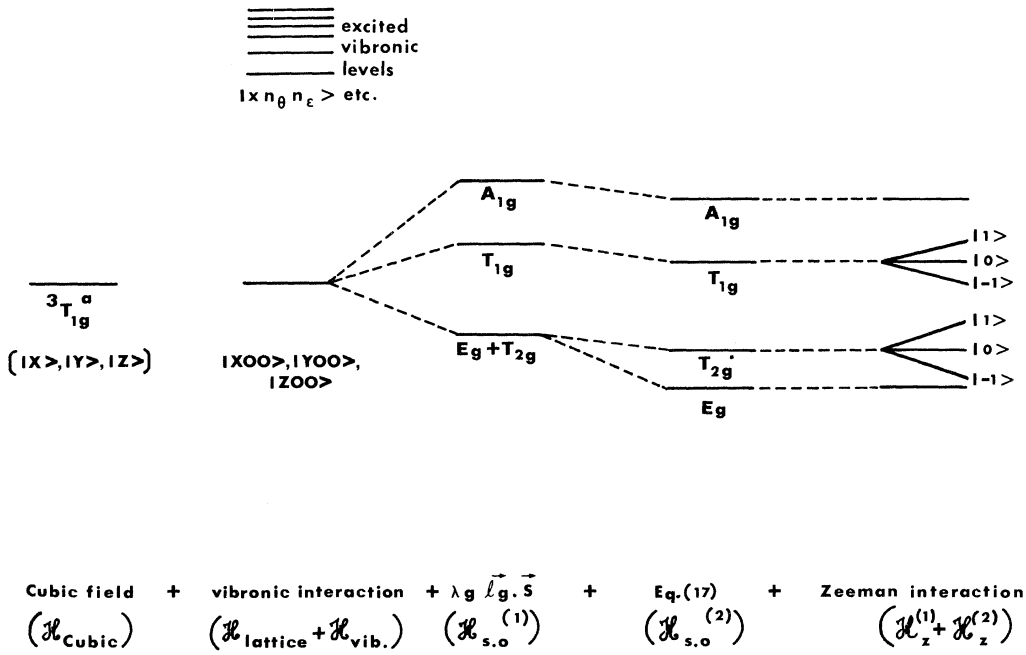

FIG. 2. The low-lying vibronic energy levels of the V^{3+} ion at cubic site in MgO with spin-orbit interaction.

$$\times[(l_{gx}l_{gy}+l_{gy}l_{gx})(s_xH_y+s_yH_x)$$
$$+(l_{gy}l_{gz}+l_{gz}l_{gy})(s_yH_z+s_zH_y)$$
$$+(l_{gz}l_{gx}+l_{gx}l_{gz})(s_zH_x+s_xH_z)]\ ,$$

where

$$g_1=-\frac{2\alpha K\lambda_{\rm eff}}{\hbar\omega_E}\exp(-3x)\,G(3x)$$

and

$$g_2=-\frac{\alpha K\lambda_{\rm eff}}{\hbar\omega_E}\exp(-3x)\,G(3x/2)\ . \tag{24}$$

The terms nonlinear in H are neglected because they are of much smaller magnitude. We shall now study the effect of the Zeeman interaction on the spin-orbit states.

E_g: Within this lowest spin-orbit doublet neither $\mathcal{H}_x^{(1)}$ nor $\mathcal{H}_x^{(2)}$ has any nonvanishing matrix elements. Consequently the magnetic field causes no splitting of this doublet.

T_{2g}: Operating $\mathcal{H}_x$ [Eq. (22)] on the three states of this triplet we get the following determinant:

$$\begin{vmatrix} 0 & i\beta H_x[(1+\frac{1}{2}\gamma)+g_2] & 0 \\ -i\beta H_x[(1+\frac{1}{2}\gamma)+g_2] & 0 & 0 \\ 0 & 0 & 0 \end{vmatrix}\ . \tag{25}$$

The eigenfunctions and the eigenvalues of this determinant are

$$|T_{2g}^3\rangle : 0\ ,$$
$$\frac{1}{\sqrt{2}}(|T_{2g}^1\rangle - i|T_{2g}^2\rangle) : \beta H_x(1+\tfrac{1}{2}\gamma+g_2)\ , \tag{26}$$
$$\frac{1}{\sqrt{2}}(|T_{2g}^1\rangle + i|T_{2g}^2\rangle) : -\beta H_x(1+\tfrac{1}{2}\gamma+g_2)\ ,$$

where the states $|T_{2g}^i\rangle$ are those given in Eq. (20). Using the spin-Hamiltonian formalism, we can describe the above three states as the $|0\rangle$, $|1\rangle$ and $|-1\rangle$ states of an effective spin $S=1$ and their energies by an effective spin Hamiltonian $g\beta H_xS_x$, so that we have

$$g=1+\tfrac{1}{2}\gamma+g_2\ . \tag{27}$$

This result will not change for the magnetic field along x or y direction because the symmetry is cubic.

T_{1g}: In analogy with the case of the T_{2g} triplet we can show that the triplet T_{1g} can be characterized by an effective spin $S=1$ and a spin Hamiltonian $g\beta H_xS_x$ where

$$g=1+\tfrac{1}{2}\gamma-g_2\ , \tag{28}$$

the three states being T_1^3, $(1/\sqrt{2})(|T_1^1\rangle+i|T_1^2\rangle)$, and $(1/\sqrt{2})(|T_1^1\rangle-i|T_1^2\rangle)$. Figure 2 shows the nature of the magnetic field splittings of the spin-orbit states.

D. Transitions Induced within Zeeman States by Acoustic Waves

In APR experiments sound waves are propagated within the crystal which will cause periodic displacements of the ions and these are coupled to the spin of the impurity ion through orbit-lattice and spin-orbit interactions.[14] These displacements in the molecular cluster model are related to the symmetry-adapted displacements of the cluster.

Within the electronic triplet $^3T_{1g}^a$ the Hamiltonian for the sound waves[3] can be written in the same form as in Eq. (9),

$$\mathcal{H}_{\rm sound}=[V_E(\bar{Q}_\theta\mathcal{E}_\theta+\bar{Q}_\epsilon\mathcal{E}_\epsilon)$$
$$+V_T(\bar{Q}_\xi\mathcal{T}_\xi+\bar{Q}_\eta\mathcal{T}_\eta+\bar{Q}_\zeta\mathcal{T}_\zeta)]\cos\omega t\ , \tag{29}$$

where ω is the frequency of the sound waves and the $\bar{Q}_i$ are the symmetry-adapted displacements of the ions in the cluster due to the sound waves. For sound waves with propagation vector $\vec{K}$ and polarization $\vec{p}$ having direction cosines l_1, m_1, n_1 and l_2, m_2, n_2, respectively, with respect to the crystal axes, we can write[15,2]

$$\bar{Q}_\theta=\frac{\epsilon R}{\sqrt{3}}(2n_1n_2-m_1m_2-l_1l_2)\ ,$$
$$\bar{Q}_\epsilon=\epsilon R(m_1m_2-l_1l_2)\ ,$$
$$\bar{Q}_\xi=\epsilon R(m_1n_2+m_2n_1)\ , \tag{30}$$
$$\bar{Q}_\eta=\epsilon R(n_1l_2+n_2l_1)\ ,$$
$$\bar{Q}_\zeta=\epsilon R(l_1m_2+l_2m_1)\ .$$

Here ϵ is the strength of the strain due to the acoustic waves and R is the distance of the nearest O^{2-} ions from the V^{3+} ion.

The probability of transition induced by the acoustic waves within the Zeeman states is estimated directly by calculating the matrix elements of $\mathcal{H}_{\rm sound}$ between the actual Zeeman states or alternatively one can construct an effective spin Hamiltonian for the acoustic waves and then calculate the matrix elements of this effective Hamiltonian between the Zeeman states expressed in terms of an effective spin S. The latter procedure is more convenient for the study of the line shape and consequently we adopt it here. The ground E_g doublet is nonmagnetic and hence it does not participate in the resonance experiments. We therefore consider the next excited triplet T_{2g}.

The effective spin Hamiltonian for the sound waves $\mathcal{H}_{\rm dyn}$, within this triplet described by an effective spin $S=1$, is given by[15,16]

$$\mathcal{H}_{\rm dyn}=\left\{\frac{\sqrt{3}}{4}\frac{G_{11}}{R}[(2S_z^2-S_x^2-S_y^2)\bar{Q}_\theta+\sqrt{3}(S_x^2-S_y^2)\bar{Q}_\epsilon]\right.$$

$$+\frac{G_{44}}{R}\left[(S_yS_z+S_zS_y)\bar{Q}_\xi+(S_zS_x+S_xS_z)\bar{Q}_\eta+(S_xS_y+S_yS_x)\bar{Q}_\zeta\right]\Big\}\cos\omega t\ , \quad (31)$$

where G_{11} and G_{44} are the magnetoelastic constants. These can be expressed in terms of V_E and V_T by equating any of the matrix elements of $\mathcal{H}_{\rm dyn}$ within the effective spin states $|0\rangle$, $|1\rangle$, and $|-1\rangle$ with the corresponding element of $\mathcal{H}_{\rm sound}$ within the actual Zeeman states given in Eq. (26). Thus, we obtain

$$G_{11}=(1/\sqrt{3})\,V_E R \quad \text{and} \quad G_{44}=\tfrac{1}{2}\,V_T R\exp(-\tfrac{3}{2}x)\ , \quad (32)$$

where the exponential factor arises from the reduction of the T_{2g}-type operator inside the vibronic ground level due to orbital coupling with the E_g modes only. Let us now consider the transitions induced by $\mathcal{H}_{\rm dyn}$ when the Zeeman field is along [001] and the longitudinal sound waves are propagated in an arbitrary direction $[l_1 m_1 n_1]$.

(i) $\Delta m_s=\pm 1$, i.e., transitions $|0\rangle\rightarrow|1\rangle$ and $|-1\rangle\rightarrow|0\rangle$: The resonance condition for these transitions is $\hbar\omega=g\beta H$, where g is given by Eq. (27). The intensity of this line will be proportional to

$$|\langle 0|\mathcal{H}_{\rm dyn}|1\rangle|^2=\frac{1}{2}\,\frac{G_{44}^2}{R^2}(Q_\xi^2+Q_\eta^2)\ . \quad (33)$$

It is evident from Eqs. (30) that in the case of longitudinal waves propagating along [100] or [010], $\bar{Q}_\xi=\bar{Q}_\eta=\bar{Q}_\zeta=0$, so that, in neither of these cases will $\Delta m_s=\pm 1$ transitions be observed. For the sound waves in any other direction in the [110] plane $\bar{Q}_\zeta$ is nonzero, but no resonance due to $\Delta m_s=\pm 1$ transitions is observed because this particular component of the T_{2g}-type displacements does not participate in this transition, as is evident from Eq. (31). For any direction of propagation other than in the [110] plane, although the transition is allowed the intensity will be very small due to the small magnitude of G_{44}.

(ii) $\Delta m_s=\pm 2$, i.e., the transitions $|-1\rangle\rightarrow|1\rangle$: The resonance condition in this case is $\hbar\omega=2g\beta H$, where g is same as before. The intensity of this line is proportional to

$$|\langle 1|\mathcal{H}_{\rm dyn}|-1\rangle|^2=\frac{1}{R^2}\left(\tfrac{9}{16}\,G_{11}^2\bar{Q}_\epsilon^2+G_{44}^2\bar{Q}_\zeta^2+\tfrac{3}{2}G_{11}G_{44}\bar{Q}_\epsilon\bar{Q}_\zeta\right)\ . \quad (34)$$

When the longitudinal acoustic waves are propagated in [100] or [010] then the intensity is proportional to G_{11}^2 only. When the waves are along [110] the intensity will be proportional to G_{44}^2 only. Hence there will be a large decrease in the intensity of the resonance line due to the $\Delta m_s=\pm 2$ transition as the propagation direction of the sound waves is changed from [100] or [010] to [110].

E. Different Features of APR Line for V^{3+} Ion at Cubic Site

We shall now study quantitatively the different features of the spectra due to the first-excited T_{2g} level for V^{3+} ions in pure cubic sites. The zero-field separation of this level from the ground-state doublet is given by

$$D=\frac{\lambda_{\rm eff}^2}{\hbar\omega_E}\exp(-3x)[G(3x)-G(\tfrac{3}{2}x)] \quad (35)$$

and the g value of the resonance line is

$$g=1+\frac{\alpha K}{2}\exp(-\tfrac{3}{2}x)-\frac{\alpha K\lambda_{\rm eff}}{\hbar\omega_E}\exp(-3x)G(\tfrac{3}{2}x)\ . \quad (36)$$

Thus both D and g are functions of $\lambda_{\rm eff}$, $E_{\rm JT}$, and $\hbar\omega_E$. Since $\lambda_{\rm eff}=-1.2K\lambda_{\rm free\ ion}$, where K is the covalency factor, we can study the variation of D and g as functions of $E_{\rm JT}$ and $\hbar\omega_E$ for some particular values of K. In Fig. 3, we have plotted D and g against $E_{\rm JT}$ for some relevant values of $\hbar\omega_E$, taking $K=1$, i.e., assuming the covalency effects to be negligibly small. The three values of $\hbar\omega_E$, namely, 400, 450, and 500 $\rm cm^{-1}$ are chosen on the basis of the experimental results on phonon sidebands associated with the zero-phonon electronic transitions in MgO doped with Ni^{2+}, V^{2+}, Cr^{3+}, and Mn^{4+} ions.[6] It is evident from these curves that the peak in the phonon density of states occurs between 400 and 500 $\rm cm^{-1}$ in all these cases. Now taking the g value to be the more precisely known observable, we determine the range of $E_{\rm JT}$ within which $g=0.69\pm0.01$ from each of the g-vs-$E_{\rm JT}$ curves and then find the range of values for D from the corresponding D-vs-$E_{\rm JT}$ curve. We tabulate these values in Table I for three different values of K and three values of $\hbar\omega_E$ for each K. It should be noted that if we take the experimental value 10.2 ± 1.0 $\rm cm^{-1}$ as our reference for D, then as we decrease K we have to take lower values of $\hbar\omega_E$ in order to get a simultaneous fit with both g and D within the experimental uncertainties. Assuming negligible covalency effects, the simultaneous fit with g and D is obtained for $\hbar\omega_E=500$ and 450 $\rm cm^{-1}$ with the range of $E_{\rm JT}$ lying within 280–300 and 260–280 $\rm cm^{-1}$, respectively. These values of $\hbar\omega_E$ are relevant as we have already noted. Also the relative magnitudes of $E_{\rm JT}$ and $\hbar\omega_E$ seem consistent on the basis of an effective point-charge calculation (Appendix). For $K=0.9$ we obtain simultaneous fits with D and g for $\hbar\omega_E=400$ and 350 $\rm cm^{-1}$. These values are further lowered as K decreases. Hence on the basis of existing experimental data one can infer that the covalency effects are unimportant and $E_{\rm JT}$ and $\hbar\omega_E$ cannot be estimated more precisely than the values quoted in Table I. But, one can convincingly say that the experimental g value and the zero-field separation D are explained by taking proper account of the dynamical Jahn-Teller

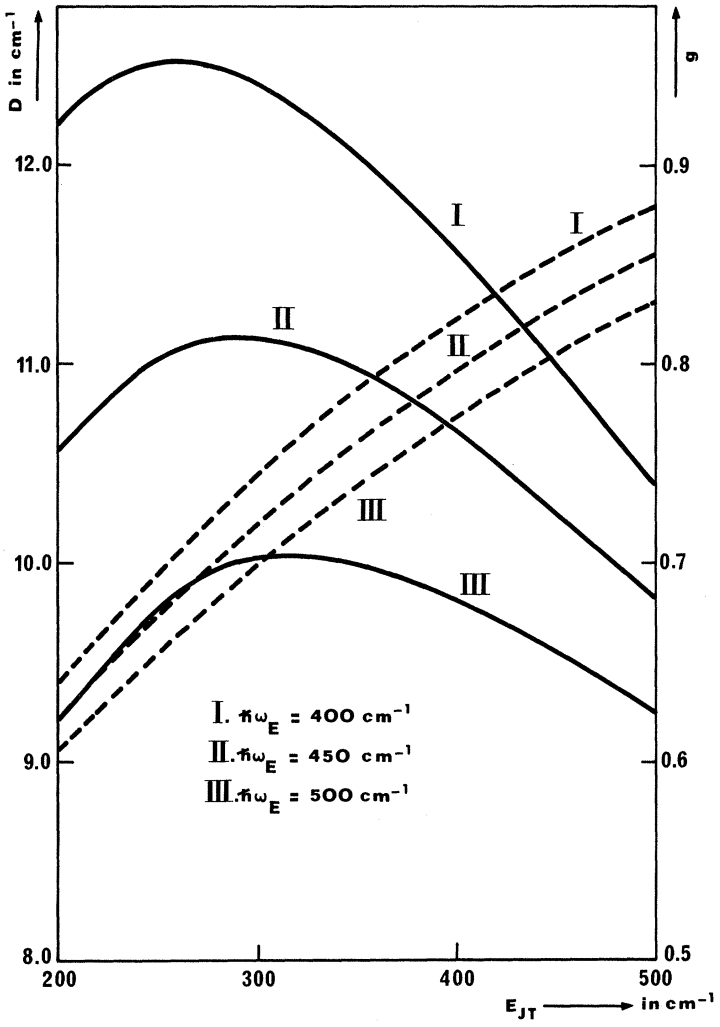

FIG. 3. The variations of g and D parameters with E_{JT} for some values of $\hbar\omega_E$ with the covalency factor $K=1$. The solid and the broken lines represent D and g, respectively.

effects within the orbital triplet $^3T_{1g}^a$ of the V^{3+} ions at cubic sites in MgO.

This model alone is, however, not sufficient to explain the broad asymmetric line shape.

Also, one should note that [from Eq. (32)]

$$G_{11}/G_{44} = (2/\sqrt{3})(V_E/V_T)\exp(\tfrac{3}{2}x) \ . \qquad (37)$$

With $V_E/V_T \sim 5.6$ and $E_{JT}/\hbar\omega_E \sim 0.6$ we get $G_{11}/G_{44} \sim 16.0$. Thus the intensity of the resonance due to $\Delta m_s = \pm 1$ will be very weak and the line which is observed corresponds to a $\Delta m_s = \pm 2$ transition. But the expression for the intensity of this line [Eq. (33)] indicates that when the sound waves are parallel to [110] then the intensity is proportional to G_{44}^2 and hence in this condition the resonance absorption is expected to be very weak. This conclusion is also not in agreement with the experimental observation. In Sec. IV, we shall see how far the line shape and the intensity of the observed resonance are explained when we take account of a small random strain field at the cubic sites.

IV. EFFECTS OF SMALL STRAIN FIELD ABOUT CUBIC SITES ON APR SPECTRA OF V^{3+} IONS IN MgO

Assuming the existence of a small strain field in an arbitrary direction about the cubic sites, we write the strain Hamiltonian in the following general form:

$$\mathcal{H}_{\text{strain}} = \frac{1}{R}\left[V_E(\mathcal{E}_\theta e_\theta + \mathcal{E}_\epsilon e_\epsilon) + V_T(\mathcal{T}_\xi e_\xi + \mathcal{T}_\eta e_\eta + \mathcal{T}_\zeta e_\zeta)\right] \ . \qquad (38)$$

The second term is neglected in the present calculations because V_T is much smaller than V_E. The symmetry-adapted strain components e_θ and e_ϵ are given by[16]

$$e_\theta = \frac{1}{\sqrt{3}}(2e_{zz} - e_{xx} - e_{yy}) \ , \qquad e_\epsilon = (e_{xx} - e_{yy}) \ . \qquad (39)$$

From the above expressions it is evident that e_θ and e_ϵ characterize distortions of tetragonal and orthorhombic type about the z axis, respectively.

TABLE I. The range of the Jahn-Teller energy E_{JT} is fixed from the g-vs-E_{JT} curves taking $g = 0.69 \pm 0.01$. The column for D gives the corresponding values of D within this range of E_{JT} from the D-vs-E_{JT} curves.

Covalency factor K	Energy of the E_g modes of vibration $\hbar\omega_E$(cm^{-1})	Jahn-Teller energy E_{JT}(cm^{-1})	g value	Zero-field separation D(cm^{-1})
	500.0	289.0 ± 11.0	0.69 ± 0.01	9.99 ± 0.03
1.00	450.0	269.0 ± 11.0	0.69 ± 0.01	11.09 ± 0.03
	400.0	246.0 ± 10.0	0.69 ± 0.01	>12.5
	400.0	237.0 ± 9.0	0.69 ± 0.01	9.67 ± 0.02
0.88	350.0	212.0 ± 6.0	0.69 ± 0.01	11.04 ± 0.02
	300.0	193.0 ± 7.0	0.69 ± 0.01	>12.8
	350.0	209.0 ± 9.0	0.69 ± 0.01	9.13 ± 0.03
0.80	300.0	187.0 ± 7.0	0.69 ± 0.01	10.66 ± 0.01
	250.0	164.0 ± 6.0	0.69 ± 0.01	>12.7

These strain fields would cause splittings of the order of 1 cm^{-1} and hence we can consider the Hamiltonian in Eq. (38) as a perturbation on the spin-orbit states. In the present analysis, we shall consider the effect of the strain Hamiltonian on the T_{2g} vibronic spin-orbit triplet state only. The three components of the T_{2g} level which were degenerate for a site of cubic symmetry [Eq. (20)] will split up into three separate levels due to $\mathcal{H}_{\text{strain}}$ and their energies will be given by

$$\begin{aligned} T_{2g}^1 &: (V_E/4R)\,(-e_\theta + \sqrt{3}e_\epsilon)\,, \\ T_{2g}^2 &: (V_E/4R)\,(-e_\theta - \sqrt{3}e_\epsilon)\,, \\ T_{2g}^3 &: (V_E/2R)\,e_\theta\,, \end{aligned} \tag{40}$$

with reference to their spin-orbit energy given in Eqs. (30). As in the cases of $\mathcal{H}_{\text{Zeeman}}$ and $\mathcal{H}_{\text{sound}}$ we can also express the strain interaction as an effective Hamiltonian acting within the triplet state described by an effective spin $S = 1$. This has the form

$$\mathcal{H}_{\text{spin(strain)}} = \delta(3S_z^2 - S(S+1) + E(S_x^2 - s_y^2)\,, \tag{41}$$

assuming the z axis to be the direction of the tetragonal distortion. From the equivalence of the two expressions given in Eqs. (38) and (41), one can show that

$$\delta = -(V_E/4R)\,e_\theta$$

and

$$E = (\sqrt{3}/4)\,(V_E/R)\,e_\epsilon\,. \tag{42}$$

Both δ and E vary randomly. For orthorhombic strains, x, y, and z directions are all nonequivalent and consequently if the Zeeman field is taken along any of the cubic axis, e.g., along [001], and δ and E are taken to be arbitrary parameters, then the following effective spin Hamiltonian would account for all the ions in the crystal. This spin-Hamiltonian would act on the spin-orbit triplet state [Eq. (20)] and is given by

$$\mathcal{H}_{\text{spin}} = g_{\parallel}\beta H S_z + \delta\,[3S_z^2 - S(S+1)] + E(S_x^2 - S_y^2)\,. \tag{43}$$

The resulting eigenstates and their eigenvalues are

$$\begin{aligned} \psi_1 &= |1\rangle\cos\theta + |-1\rangle\sin\theta : \delta + (g_{\parallel}^2\beta^2H^2 + E^2)^{1/2}\,, \\ \psi_2 &= |1\rangle\cos\theta - |-1\rangle\sin\theta : \delta - (g_{\parallel}^2\beta^2H^2 + E^2)^{1/2}\,, \\ \psi_3 &= |0\rangle \qquad\qquad\qquad\quad : -2\delta\,, \end{aligned} \tag{44}$$

where

$$\tan\theta = [(g_{\parallel}^2\beta^2H^2 + E^2)^{1/2} - g_{\parallel}\beta H]/E\,.$$

Now as the acoustic waves of frequency ω are propagated within the crystal in an arbitrary direction, the following transitions are induced:

$\Delta m_s = \pm 2$. From Eq. (31), the resonance condition for these transitions is

$$\hbar\omega = 2(g_{\parallel}^2\beta^2H^2 + E^2)^{1/2}. \tag{45}$$

From Eq. (31) the probability of these transitions comes out to be proportional to

$$|\langle\psi_1|\mathcal{H}_{\text{dyn}}|\psi_2\rangle|^2 = \frac{1}{R^2}\,(\tfrac{9}{16}G_{11}^2\,\overline{Q}_\epsilon^2 + G_{44}^2\,\overline{Q}_\xi^2 + \tfrac{3}{2}G_{11}G_{44}\,\overline{Q}_\epsilon\,\overline{Q}_\xi)(\cos^2\theta - \sin^2\theta)^2\,. \tag{46}$$

From Eq. (45), we see that for any direction of propagation of the acoustic waves, the maximum resonance field is needed for those ions for which there is no orthorhombic distortion. The intensity of the resonance line also attains the peak value at $E = 0$, because then $\tan\theta = 0$. The g value corresponding to the peak of the absorption line is $g_{\parallel} = g_{\text{cubic}}$. The strain field has a distribution on either side of the cubic field ($E = 0$), but the quadratic power of E in Eq. (45) ensures that the resonance line has a sharp cutoff on the high-field side. On the low-field side there will be a long tail because all the ions with $E \neq 0$ will contribute to the resonance line. The intensity falls off as E increases, becoming zero as E reaches the value $\hbar\omega/2$, which is of the order of 0.15 cm^{-1}.

It should also be noted that the intensity of the resonance line is proportional to $(9/16R^2)\,G_{11}^2\overline{Q}_\epsilon^2$

$\times(\cos^2\theta - \sin^2\theta)^2$ when the direction of propagation of the acoustic waves is along [100] or [010]. But as the propagation direction is changed to [110], the intensity of this particular line becomes proportional to G_{44}^2 and is small.

$\Delta m_s = \pm 1$. The resonance condition for these transitions is

$$\hbar\omega = 3\delta \pm (g_{\parallel}^2 \beta^2 H^2 + E^2)^{1/2} \tag{47}$$

and the propability of transitions is proportional to [from Eq. (31)]

$$|\langle\psi_1|\mathcal{H}_{\rm dyn}|\psi_3\rangle|^2 = \frac{G_{44}^2}{2R^2}[(\cos\theta - \sin\theta)^2 \overline{Q}_\xi^2 + (\cos\theta + \sin\theta)^2 \overline{Q}_\eta^2] . \tag{48}$$

For the acoustic waves propagating in the xy plane these transitions are not allowed. For any general direction of propagation of the acoustic waves away from the xy plane, the resonance is allowed but it is difficult to detect it because the line suffers a large broadening due to the distribution in δ and also because it has a very low intensity, the absorption being proportional to G_{44}^2.

It is seen from Eq. (45) that the tetragonal distortion does not enter into the resonance condition for the $\Delta m_s = \pm 2$ transitions. So the ions with different values of δ contribute to the APR signal, but the orthorhombic field E determines the shape of the line.

V. DISCUSSION

First, let us see whether the magnitude of the hyperfine interaction parameter A, which was found experimentally to be 0.0042 cm^{-1}, is explained by the model presented in this paper. The basic hyperfine-interaction Hamiltonian operating on the orbital ground state ^3F of the V^{3+} ion is given by

$$\mathcal{H}_{\rm hf} = P[\vec{L}\cdot\vec{I} + \tfrac{1}{105}\{L(L+1)\vec{S}\cdot\vec{I} - \tfrac{3}{2}(\vec{L}\cdot\vec{S})(\vec{L}\cdot\vec{I}) - \tfrac{3}{2}(\vec{L}\cdot\vec{I})(\vec{L}\cdot\vec{S})\} + k\vec{S}\cdot\vec{I}] , \tag{49}$$

where $P = 2\beta\mu_N\langle 1/r^3\rangle = 0.0102$ cm^{-1}, $L = 3$, and k is the strength of the contact interaction.[17] The matrix elements of this Hamiltonian between the vibronic spin-orbit states given in Eqs. (20) should be equal to the corresponding matrix elements of the effective hyperfine Hamiltonian $A\vec{S}\cdot\vec{I}$ between the same states expressed in terms of an effective spin of unity. Thus we obtain

$$A = \tfrac{1}{2}P\{\alpha K\exp(-\tfrac{3}{2}) + \tfrac{1}{105}[12.0 - 3(\alpha K)^2\exp(-3x)] - k\} + \frac{P\alpha K\lambda_{\rm eff}}{\hbar\omega_E}\exp(-3x)G(\tfrac{3}{2}x) . \tag{50}$$

From this, one can estimate k for V^{3+} ion using the experimental value of A. With $\lambda_{\rm eff} = -125.0$ cm^{-1}, $E_{\rm JT} = 300$ cm^{-1}, $\hbar\omega_E = 450.0$ cm^{-1} and taking the covalency factor K to be unity, we get $k = 0.2$. It is hard to judge this value of k which is otherwise not known and also because the amount of admixture between the s and d orbitals of V^{3+} ions is not known. It will be interesting to calculate k for V^{3+} ion in Al_2O_3 from the observed electron-paramagnetic-resonance spectra[18] and see how this value compares to the above estimated value of k for V^{3+} ions in MgO. One would expect k not to differ much in the two cases.

We have already pointed out that due to the charge compensation of V^{3+} ions in the MgO crystal, there should be equal numbers of V^{3+} ions in the cubic and the tetragonal sites. So far we have concentrated our attention on the V^{3+} ions in the cubic sites which are shown to be responsible for the observed APR spectra. Questions may now be raised about the role of the V^{3+} ions in tetragonal sites, whether these are at all observed in the APR experiments. So, we shall now discuss briefly the theory of the Jahn-Teller interactions for V^{3+} ions at the tetragonal sites. In the presence of a static tetragonal field the vibronic orbital triplet ground state T_{1g} splits up into a doublet and a singlet, the singlet lying Δ cm^{-1} above the doublet. Next, as we consider the spin-orbit interaction on these vibronic states we find that the form of $\mathcal{H}_{\rm so}^{(1)}$ remains the same as that in Eq. (13) because the tetragonal field is diagonal within the manifold of the vibronic ground states. But the second-order interaction $\mathcal{H}_{\rm so}^{(2)}$ will be modified due to the changes in the level separations and for the case of the tetragonal field splitting Δ being less than the vibronic splitting $\hbar\omega_E$, we can write

$$\mathcal{H}_{\rm so}^{(2)} = -\frac{\lambda_{\rm eff}^2}{\hbar\omega_E}[al_{gz}^2 S_z^2 + \tfrac{1}{2}(b+e)(l_{gx}^2 S_x^2 + l_{gy}^2 S_y^2) + \tfrac{1}{2}(b-e)(l_{gz}^2 S_x^2 + l_{gz}^2 S_y^2 - l_{gx}^2 S_y^2 - l_{gy}^2 S_x^2) + c(l_{gx}l_{gy}S_xS_y + l_{gy}l_{gx}S_yS_x) + d(l_{gx}l_{gz}S_xS_z + l_{gz}l_{gx}S_zS_x + l_{gy}l_{gz}S_yS_z + l_{gz}l_{gy}S_zS_y)] , \tag{51}$$

where

$$a = \exp(-3x)G(3x) , \quad b = \exp(-3x)G(3x, f) ,$$

$$c = \exp(-3x)G(\tfrac{3}{2}x, f) ,$$

$$d = \tfrac{1}{2}\exp(-3x)[G(\tfrac{3}{2}x) + G(\tfrac{3}{2}x, -f)] ,$$

$$e = \exp(-3x)G(3x, -f) , \quad f = \Delta/\hbar\omega_E ,$$

and

$$G(x, f) = +\sum_n^{1,\infty} \frac{x^n}{n!(n+f)!} . \tag{52}$$

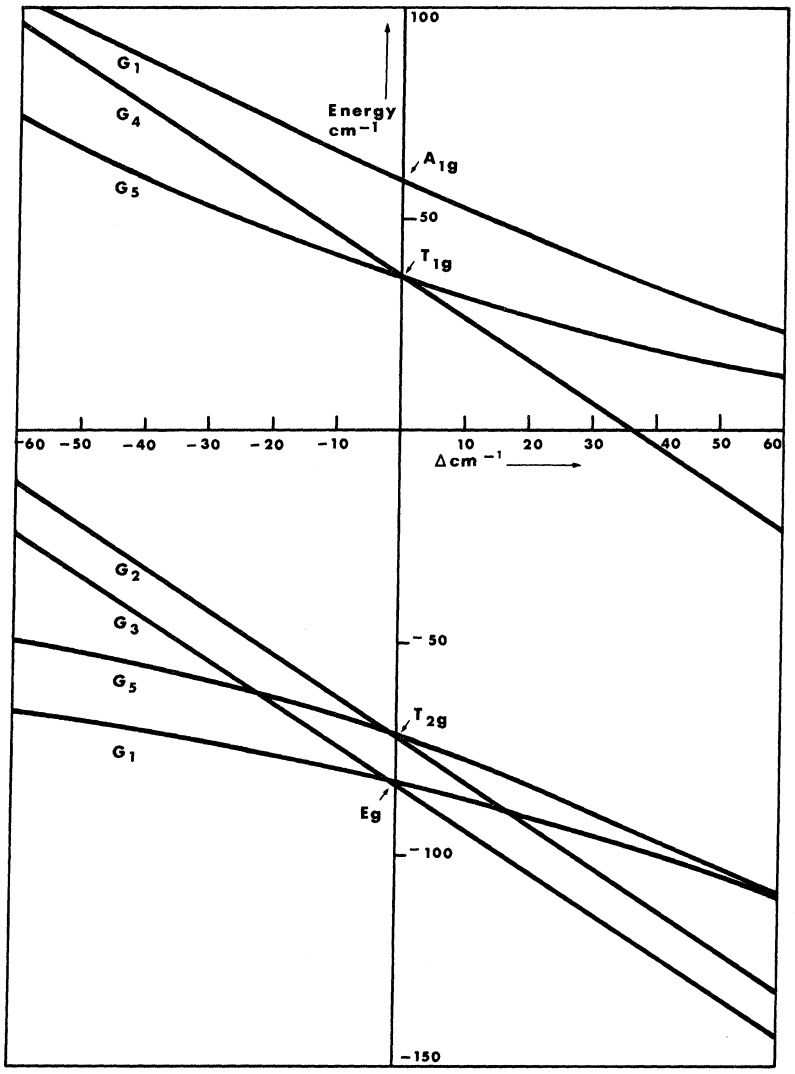

FIG. 4. The plot of the low-lying vibronic spin-orbit levels of MgO : V^{3+} against the tetragonal field parameter Δ, with $\hbar\omega_E = 450.0$ cm^{-1}, $E_{JT} = 250.0$ cm^{-1}, and the covalency parameter $K = 1$.

This expression reduces to that of Eq. (17) when the symmetry is cubic. Solving the total Hamiltonian $\mathcal{H}_T + \mathcal{H}_{so}^{(1)} + \mathcal{H}_{so}^{(2)}$ within the T_{2g} triplet, we get energy levels which are plotted graphically in Fig. 4 for the particular values of $\hbar\omega_E = 450.0$ cm^{-1} and $E_{JT} = 250.0$ cm^{-1}. These solutions are valid under the condition that Δ, the tetragonal field parameter, is less than the separation between the vibronic states $\hbar\omega_E$. For the positive values of Δ, the separation D between the ground singlet G_3 and the excited doublet G_5 goes on increasing sharply with Δ, so that even for small values of the tetragonal field D would be fairly large. For negative values of Δ, the separation D between the ground singlet G_1 and the excited doublet G_5 increases at a slower rate but since the tetragonal field Δ is expected to be of the order of -200 cm^{-1} for a positive-ion vacancy in the next-nearest position, the separation D would be too large to give rise to any observable resonance absorption. The g value for the excited doublet G_5 is given by

$$g_{\parallel} = -(1 - 0.6\exp(-\tfrac{3}{2}x))\cos 2\phi + \frac{\alpha K \lambda_{eff}}{\hbar\omega_E}\exp(-3x)\,G(\tfrac{3}{2}x)\,, \quad (53)$$

where

$$\tan\phi = \{2\lambda_g - [4\lambda_g^2 + (\lambda_2 - \lambda_1 - \Delta)^2]^{1/2}\}/(\lambda_2 - \lambda_1 - \Delta)\,.$$

The variation of $g_{\parallel}$ with Δ is shown in Fig. 5. For the variation in $\Delta \sim 1$ cm^{-1}, $g_{\parallel}$ varies 1 part in 10^3. However, for large variation in Δ, $g_{\parallel}$ changes appreciably. The strain fields around the cubic site are small and the consequent variation in the g value will be negligible and hence there will not be any significant addition to the linewidth on this account. If there be any, then this will be on the high field side. As regards the V^{3+} ions in tetragonal sites

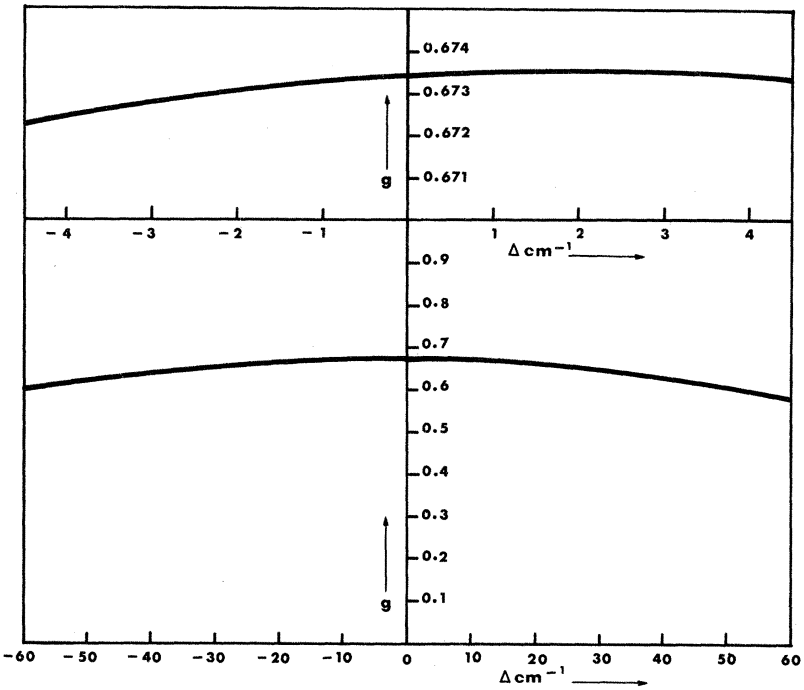

FIG. 5. The plot of g against the tetragonal field parameter Δ, corresponding to $\hbar\omega_E = 450.0$ cm^{-1}, $E_{JT} = 250.0$ cm^{-1}, and the covalency factor $K = 1$.

arising due to charge compensation mechanism, these would not be observed in the APR experiments because of the large separation of the excited doublet from the ground singlet.

We shall now discuss the different approximations made in our analysis. First, the coupling of the electronic triplet to the T_{2g} modes of vibration was neglected. This was done because (i) the magnitude of V_T is one-fifth of that of V_E and (ii) the matrix elements of the T_{2g}-type operators within the vibronic triplet ground state would be reduced by the factor $\exp(-\frac{3}{2}x)$. Second, we have not considered the second-order spin-orbit interaction arising from the excited electronic states. An order-of-magnitude calculation shows that its contribution to the spin-orbit energy is less than 1 cm^{-1} due to the fact that the first-excited electronic level lies 16 000 cm^{-1} higher and also because, the matrix elements of the spin-orbit interaction are much reduced due to the Jahn-Teller effect. Third, we have taken the spin-orbit interaction as perturbations on the vibronic levels. This should be a good approximation for V^{3+} ions in MgO where $\hbar\omega_E$, $E_{JT} > \lambda$. Therefore, the energies of the vibronic spin-orbit states given in this paper are not expected to change significantly if one diagonalizes the vibronic and the spin-orbit interactions within a large number of vibrational states.

Next, we discuss the possible experiments which can give additional confirmation of the model presented in this paper. Infrared measurements should be able to determine directly the energies of some of the excited vibronic spin-orbit states. From our calculations we find the energy separations of the excited levels with reference to the doublet ground state E_g to be 11.03, 119.6, and 142.2 cm^{-1} for the T_{2g}, T_{1g}, and A_{1g} level, respectively, corresponding to $\hbar\omega_E = 450.0$ cm^{-1}, $E_{JT} = 250.0$ cm^{-1}, and $\lambda_{eff} = -125.0$ cm^{-1}. One should be able to determine the last three basic parameters if infrared work provides information about these energy-level separations. The strain-field distribution about the cubic sites should cause broadening of the infrared transitions. Additional infrared lines might be detected from the V^{3+} ions in noncubic sites due to compensating charges. These correspond to the energy levels plotted graphically in Fig. 4.

As regards the direct electron-paramagnetic-resonance transitions one might investigate the possibility of using a sufficiently high magnetic field (~100 kG) to bring one of the components of the G_5 doublet within detectable range from the ground E_g level. Also, APR experiments with V^{3+} ions in other cubic crystals such as CaO, BaO, or SrO would be interesting in view of the fact that $\hbar\omega_E$ and E_{JT} will have values different from those of MgO: V^{3+}. Measurements on the thermal conductivity should also give information about the excited T_{2g} triplet.

In conclusion, it is once again emphasized that to explain the APR results on MgO: V^{3+} a model has been worked out where (i) the vibronically induced spin-orbit interactions in V^{3+} ions at the cubic sites are shown to be responsible for the g and D param-

eters and (ii) a strain field of the orthorhombic and the tetragonal nature about the cubic sites determine the unusual lineshape. It should further be noted that the physical aspects of the model do not depend on the accuracy of the experimentally determined parameters g and D. Even if one questions the precision in the determination of the zero-field separation D, the only change in the present analysis will be in the range of values of E_{JT} in Table I.

APPENDIX: ESTIMATE OF DIFFERENT PARAMETERS ON BASIS OF EFFECTIVE POINT-CHARGE MODEL

In the effective point-charge model each of the neighboring O^{2-} ions around a V^{3+} ion is assumed to have a charge Ze where Z takes partial account of the overlap and covalency effects and is different from -2. In the present case we have estimated Z from the experimental value of the cubic crystalline parameter Dq. We have $Dq = Ze^2\langle r_0^4\rangle/6R^5 = 1707$ cm^{-1} for $MgO:V^{3+}$.[7] Taking $\langle r_0^4\rangle = 0.425$ Å^4,[19] and $R = 2.1$ Å we get $Z = -5.9$ and with this value of Z we shall now calculate V_E, E_{JT}, G_{11}, and G_{44}.

(i) V_E and V_T: Expressing the orbit-lattice Hamiltonian in the form

$$\mathcal{H}_{ol} = \sum_l A_{1,\alpha} r^1 \sum_i Y_1(\Gamma_\alpha^i)\, Q(\Gamma_\alpha^i) \qquad \text{(A1)}$$

and equating its matrix elements within the T_{1g}^a electronic triplet with those of the vibrational Hamiltonian $\mathcal{H}_{vib}$ [Eq. (9)], we get

$$V_E = -\frac{\sqrt{3}Ze^2}{7}\left(-\frac{12}{5}\frac{\langle r_0^2\rangle}{R^4} + \frac{25}{6}\frac{\langle r_0^4\rangle}{R^6}\right)$$

and

$$V_T = \frac{Ze^2}{7}\left(-\frac{3}{5}\frac{\langle r_0^2\rangle}{R^4} + 5\frac{\langle r_0^4\rangle}{R^6}\right). \qquad \text{(A2)}$$

The ratio V_E/V_T is independent of Z and is equal to -5.6 with $\langle r_0^4\rangle$ and R having the values quoted earlier and $\langle r_0^2\rangle = 0.455$ Å^2.[19] The Jahn-Teller energy involves the quadratic powers of V_E and V_T and so in our analysis we have neglected the coupling of the orbital triplet to the T_{2g} modes of vibration. From Eq. (A2), we get $V_E = 1.73\times10^{-4}$ erg/cm.

(ii) E_{JT}: Substituting the above value of V_E in the expression for E_{JT}, viz., $E_{JT} = V_E^2/2\mu\omega_E^2$, where μ is the mass of the oxygen atom, we get $E_{JT} = 315$ and 400 cm^{-1} corresponding to $\hbar\omega_E = 500$ and 450 cm^{-1}, respectively.

Thus we find that the values $\hbar\omega_E = 500$ cm^{-1} and $E_{JT} = (289 \pm 11.0)$ cm^{-1} in Table I are closest to the above estimates made in the effective point-charge model. But in view of the approximations, no emphasis should be put on these definite quantitative results. They do, however, give an idea of the order of the magnitude of the different parameters involved in the theory.

(iii) G_{11} and G_{44}: On the basis of the effective point-charge model for the oxygen ions we get

$$G_{11} = V_E R/\sqrt{3} \simeq 10^4 \text{ cm}^{-1}$$

and

$$G_{44} = V_T R \exp(-\tfrac{3}{2}x)/2 \simeq 600 \text{ cm}^{-1}.$$

The above value of G_{11} may be compared to that quoted by Brabin-Smith and Rampton[1] as being greater than 2×10^3 cm^{-1}.

[1] R. G. Brabin-Smith and V. W. Rampton, J. Phys. C 2, 1759 (1969).

[2] C. A. Bates, L. C. Goodfellow, and K. W. H. Stevens, J. Phys. C 3, 1831 (1970).

[3] F. S. Ham, Phys. Rev. 138, A1727 (1965).

[4] T. Ray (unpublished).

[5] F. S. Ham, W. M. Schwarz and M. C. M. O'Brien, Phys. Rev. 185, 548 (1969).

[6] M. J. L. Sangster, thesis (University of Reading, 1968) (unpublished).

[7] M. D. Sturge, Phys. Rev. 130, 639 (1963).

[8] G. Racah, Phys. Rev. 62, 438 (1942).

[9] M. H. L. Pryce and W. A. Runciman, Discussions Faraday Soc. 26, 34 (1958).

[10] C. J. Ballhausen, *Introduction to Ligand Field Theory* (McGraw-Hill, New York, 1962), p. 28.

[11] B. Henderson and J. E. Wertz, Advan. Phys. 17, 749 (1968).

[12] J. E. Wertz and P. Auzins, Phys. Rev. 106, 484 (1957).

[13] K. W. H. Stevens, J. Phys. C 2, 1934 (1969).

[14] S. A. Altshuler, Dokl. Akad. Nauk SSSR 85, 1235 (1952).

[15] W. I. Dobrov, Phys. Rev. 134, A734 (1964).

[16] N. S. Shiren, in *Proceedings of the XIth Colloque Ampère, Eindhoven*, 1962, edited by J. Smidt (Interscience, New York, 1963).

[17] B. Bleaney and K. W. H. Stevens, Rept. Progr. Phys. 16, 109 (1953).

[18] G. M. Zverev and A. M. Prokhorov, Zh. Eksperim. i Teor. Fiz. 34, 1023 (1958); 38, 441 (1960) [Sov. Phys. JETP 7, 707 (1958); 11, 330 (1960)].

[19] F. M. O. Michel-Calendini and M. R. Kibler, Theoret. Chim. Acta (Berlin), 70, 367 (1968).